COMPARISON OF MODAL IDENTIFICATION TECHNIQUES USING A HYBRID-DATA APPROACH

Richard S. Pappa

Structural Dynamics Branch

NASA Langley Research Center

Hampton, Virginia 23665

First NASA/DOD CSI Technology Conference

November 18-21, 1986

INTRODUCTION

Modal identification is the process of determining the modal parameters (natural frequencies, damping factors, mode shapes, and modal masses) of a structure from experimental measurements. In general, these parameters are not directly measurable quantities. A commonly used approach is to infer their values from a set of measured frequency response functions (FRFs). This parameter identification process, though relatively straightforward in principle, is often quite difficult and time-consuming in practice, particularly for large or built-up structures. Large structures may have many local modes in the frequency range of interest, making it difficult to determine global characteristics at nearby frequencies. And built-up structures, consisting of two or more components connected together with fasteners or joints, are often nonlinear due to imperfect load paths across the connections.

For these structures, it may be difficult to determine the true number of modes, and many of the identified mode shapes may be questionable. Identification results can vary considerably using different analysis techniques.

Many different approaches are possible for the identification of structures (e.g., Refs. 1-7). Some work has been done on comparing various techniques mathematically (Refs. 8-9). However, virtually no information is yet available on how the techniques compare in practice. Theoretical considerations, of course, form the foundation of any technique. Unfortunately, however, the performance actually observed in practice can be affected significantly by a number of factors not accounted for explicitly in most techniques. These factors include nonlinearities, unusually high modal density or damping, local modes, unmeasured excitations, large differences in modal response amplitudes, nonstationarity, sensor noise, off-axis sensor response, signal-processing biases, inconsistent data, finite dynamic range, and roundoff error, among others.

This paper discusses a new method for studying the performance of various identification techniques in practice. The procedure is analogous to using simulated data corrupted by random noise--a commonly used procedure--except now the simulated data is "corrupted" instead with a set of complex experimental data. For this study, a set of 128 frequency response functions from an erectable truss structure with high modal density and significant nonlinearity was used. These data were modified numerically by adding two artificial modes with known parameters. The resulting "hybrid data" were then analyzed using both the Polyreference technique (Refs. 10-13) and the Eigensystem Realization Algorithm (ERA) (Refs. 14-17) over a wide range of analysis orders (i.e., assumed number of modes). Identification performance is studied by comparing the identified parameters for the artificial modes with their known values. Six different cases, using distinct and then repeated eigenvalues at three different response amplitudes, were analyzed. Representative portions of the results are discussed.

CONSTRUCTION OF "HYBRID DATA"

Figure 1 illustrates the construction of a typical "hybrid" frequency response function. The top plot shows individual FRFs for each of two simulated modes. In this case (referred to later as Case 2) the modes have natural frequencies of 50 and 55 Hz, modal damping factors of 0.5 percent, residue amplitudes of 1.0, and residue phase angles of 1.571 rad.

The middle plot in Figure 1 shows a driving-point FRF measured during a modal survey test of the erectable truss structure. More than thirty resonances appear between 10 and 128 Hz. This relatively wide frequency band was chosen for the test because there are only four or five global bending and torsion modes of the structure in the interval. The remaining resonances are associated with local modes of individual members of the truss, modes of the suspension cables, rigid-body modes, and harmonics of lower frequencies arising from nonlinearities.

The bottom plot shows the corresponding hybrid function constructed by summing the top and middle functions shown in the figure. In this case the two added modes are large enough in amplitude to rise moderately above the original experimental data. Two other modal amplitudes were also used in the study: one in which both modes were ten times larger in amplitude than those shown in Figure 1, and the other in which they were ten times smaller.

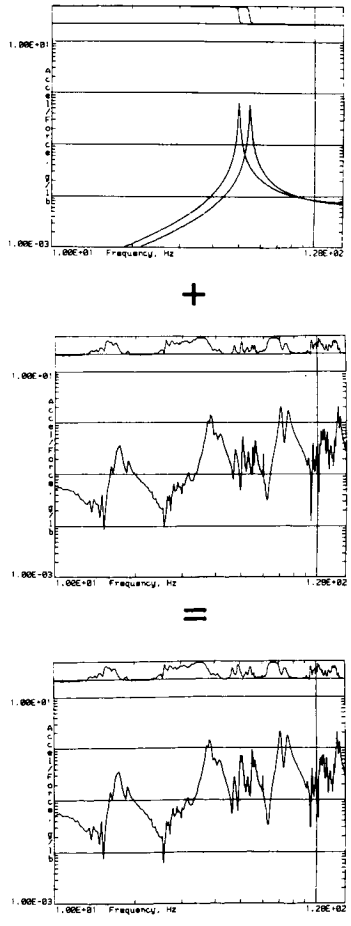

Figure 1

GENERIC 1/4-SCALE SPACE STATION TRUSS

Figure 2 shows the truss structure from which the experimental data for this study were obtained. It is a generic quarter-scale model of a configuration being considered for the Space Station. The structure is 26-1/4 feet (8.0 m) long, 3-3/4 feet (1.14 m) wide, and was suspended by two steel cables about 30 feet (9 m) long attached near the node points of the first global bending mode. The test was conducted using dual-shaker, burst-random excitation (Ref. 18), with vertical excitation applied at one end while lateral excitation was applied simultaneously at the other. Response measurements were made in the Y and Z directions (see Figure 2(b)) at each of the 32 joints using a roving set of eight accelerometers. The Hv method (Ref. 19) and one hundred averages were used in generating the set of frequency response functions.

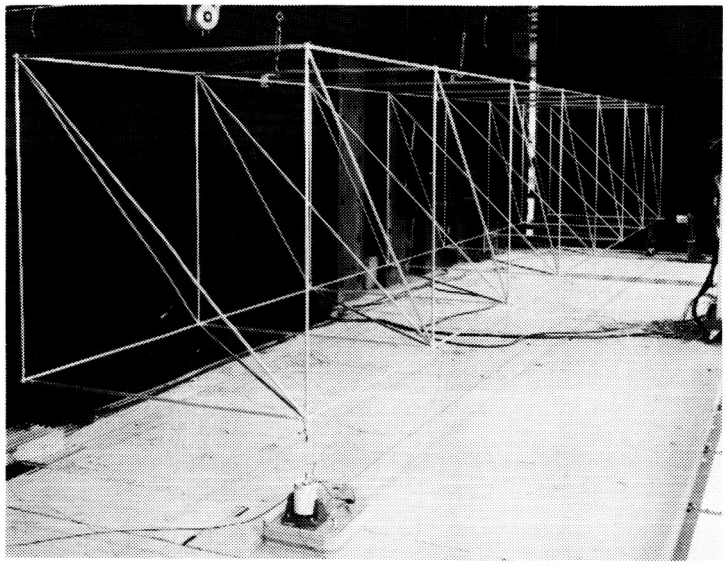

(a) Test Configuration

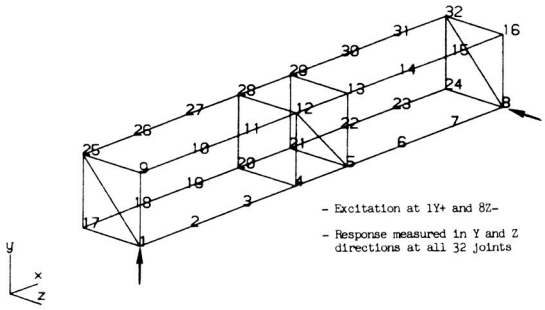

(b) Measurement Positions

Figure 2

NONLINEARITY STUDY

As mentioned earlier, the truss exhibited significant nonlinearity and high modal density. Figures 3 and 4 illustrate these characteristics. The frequency response functions shown in Figure 3 were measured at the lateral driving point using four different excitation amplitudes ranging from 0.01 lb rms at each shaker to 1.0 lb rms at each shaker. If the structure were linear, these four functions would be identical. However, considerable differences are observed. The two resonances near 70 Hz, in particular, change drastically as the amplitude is varied. Closer examination shows that most of the other resonances change as well, both in frequency and in damping level. An excitation amplitude of 0.1 lb rms at each shaker was used to acquire the data discussed in the remainder of the paper.

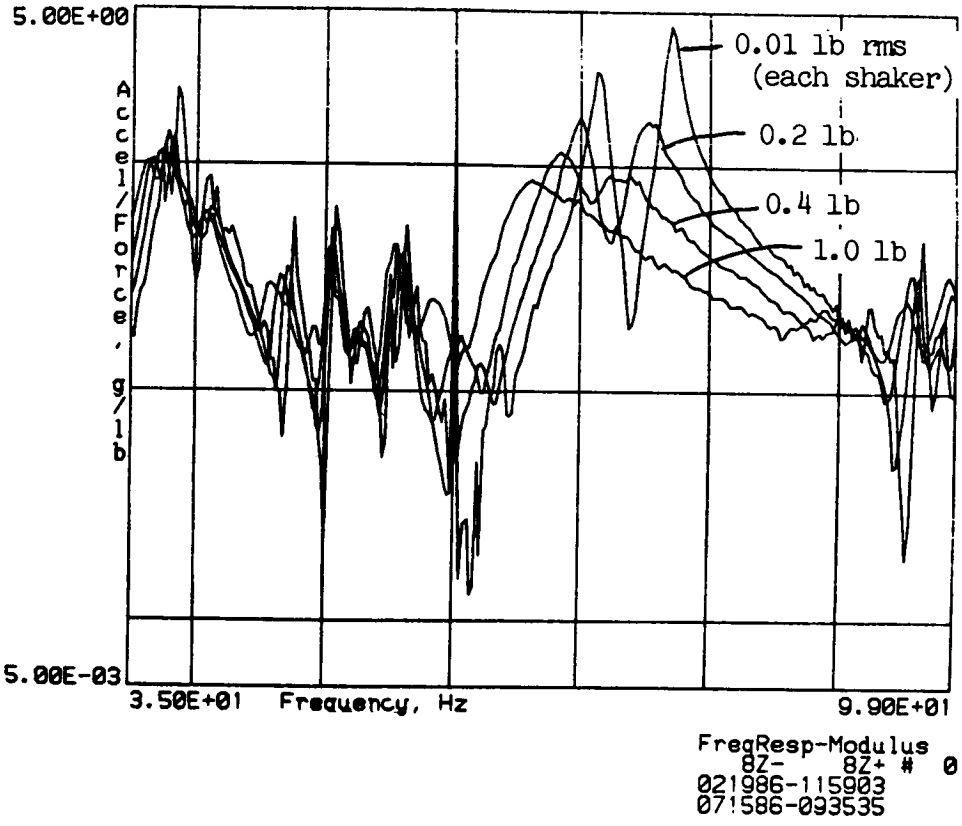

Figure 3

ESTIMATED NATURAL FREQUENCIES USING "SEARCH-FOR-PEAKS" TECHNIQUE

Figure 4 provides a quick overview of the high modal density exhibited by the truss. This plot contains 128 horizontal lines, one for each FRF which was measured. A simple "search-for-peaks" procedure (Ref. 20) was used to detect peaks occurring in each frequency response function, and the results are plotted using small tic marks. For simple, linear structures the figure would display a straight, vertical line at each natural frequency. For this data set, however, several discrepancies from this ideal behavior are observed. One discrepancy is the seemingly random scatter of peaks in the frequency interval from approximately 50 to 55 Hz. Another is that the mode near 75 Hz shifts abruptly in frequency at two different places.

The resonances between 50 and 55 Hz correspond to local resonances of the individual members of the truss. The shifts in the 75-Hz peak correspond to times during data acquisition when the eight accelerometers were moved. Whenever sensors are moved over a structure, the varying mass loading can cause frequency shifts. Miniature accelerometers were used in the test to minimize this effect, and no frequency shifting is evident except for the 75-Hz mode. It is also possible that slight variations in excitation amplitude may have occurred unintentionally during the test when the accelerometers were moved from one set of positions to the next.

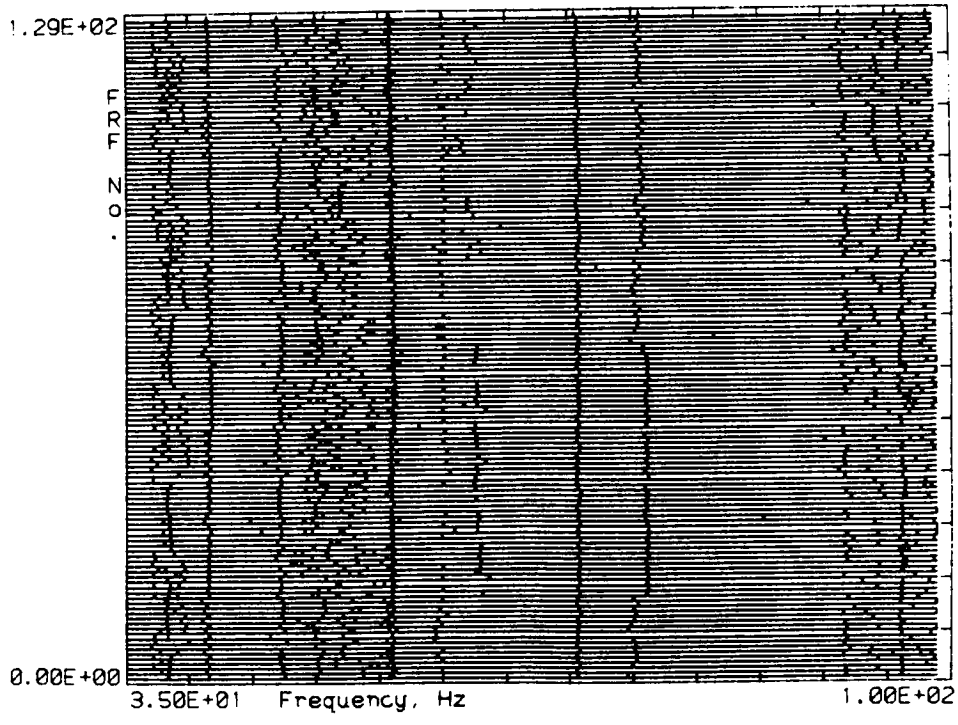

Figure 4

MODAL PARAMETERS AND MODE SHAPES FOR ARTIFICIAL MODES

The modal parameters and mode shapes used in constructing the two artificial modes, for each of six cases, are shown in Figure 5. Natural frequencies of 50 and 55 Hz were arbitrarily selected for Cases 1 through 3. The only change made in going from Case 1 to Case 3 was a reduction in residue amplitude from 10.0, to 1.0, to 0.1. The parameters chosen for Cases 4 through 6 are the same as those for Cases 1 through 3, respectively, except that the frequency of the second mode was lowered to 50 Hz. This change generated a repeated eigenvalue for these three cases.

Mode shapes for the two added modes were also arbitrarily selected. The simple alternating pattern of +1 and -1 shown in Figure 5(b) was used.

Modal Parameters, CASE 1

Label	Freq	Damping	Amplitude	Phase	Ref	Res	Mode	Flags
1	50.000	0.00500	10.00	1.571	1Y+	1Y+	1	0 0 0 1 1
2	55.000	0.00500	10.00	1.571	1Y+	1Y+	2	0 0 0 1 1

Modal Parameters, CASE 2

Label	Freq	Damping	Amplitude	Phase	Ref	Res	Mode	Flags
1	50.000	0.00500	1.000	1.571	1Y+	1Y+	1	0 0 0 1 1
2	55.000	0.00500	1.000	1.571	1Y+	1Y+	2	0 0 0 1 1

Distinct Eigenvalues -- Varying Amplitude

Modal Parameters, CASE 3

Label	Freq	Damping	Amplitude	Phase	Ref	Res	Mode	Flags
1	50.000	0.00500	0.1000	1.571	1Y+	1Y+	1	0 0 0 1 1
2	55.000	0.00500	0.1000	1.571	1Y+	1Y+	2	0 0 0 1 1

Modal Parameters, CASE 4

Label	Freq	Damping	Amplitude	Phase	Ref	Res	Mode	Flags
1	50.000	0.00500	10.00	1.571	1Y+	1Y+	1	0 0 0 1 1
2	50.000	0.00500	10.00	1.571	1Y+	1Y+	2	0 0 0 1 1

Modal Parameters, CASE 5

Label	Freq	Damping	Amplitude	Phase	Ref	Res	Mode	Flags
1	50.000	0.00500	1.000	1.571	1Y+	1Y+	1	0 0 0 1 1
2	50.000	0.00500	1.000	1.571	1Y+	1Y+	2	0 0 0 1 1

Repeated Eigenvalue -- Varying Amplitude

Modal Parameters, CASE 6

Label	Freq	Damping	Amplitude	Phase	Ref	Res	Mode	Flags
1	50.000	0.00500	0.1000	1.571	1Y+	1Y+	1	0 0 0 1 1
2	50.000	0.00500	0.1000	1.571	1Y+	1Y+	2	0 0 0 1 1

(a) Parameters

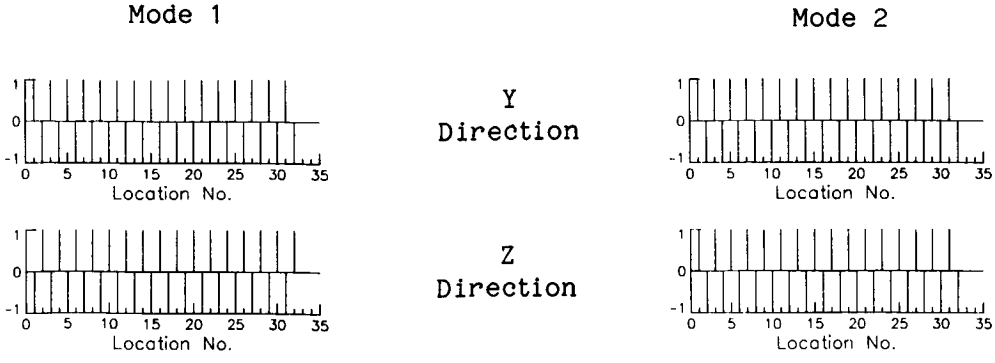

(b) Shapes

Figure 5

DATA ANALYSIS SELECTIONS

Several analysis options must be selected when using either Polyreference or ERA (see Refs. 20 and 14). It is important to recognize that considerable freedom is available to a user in choosing these analysis parameters and that the results will vary somewhat with different selections.

For this study the following choices were made: For Polyreference, a maximum mode count of 64 and a frequency interval from 35 to 99 Hz were selected; data from both references and all 64 response coordinates were accumulated into the correlation matrix; Modal Confidence Factors (MCFs) and complex residues were computed; and the assumed number of modes was incremented from 1 to 64. These selections resulted in the use of 194 time samples from each unit impulse response function.

For ERA, a block data matrix of 384 rows and 376 columns was established; data from both references (inputs) and all 64 responses (outputs) were used simultaneously, resulting in a block size of 64 by 2; time shifts of one data sample were used between all block rows, between all block columns, and between the two data matrices; a frequency interval from 35 to 99 Hz was used; and the assumed number of modes (one-half the number of retained singular values) was incremented from 1 to 64. These values were chosen so that 194 time samples were also used from each unit impulse response function.

The unit impulse response functions for both techniques were obtained by inverse Fourier transformation of the FRF data in the interval from 35 to 99 Hz (256 spectral lines).

IDENTIFICATION RESULTS

All identification results shown in this paper were generated on a VAX 11/780 computer, using Version 9.0 of Modal-Plus (Ref. 20) for all Polyreference analyses and the single-precision version of the ERA program for all ERA analyses.

To begin, the natural frequencies identified by Polyreference and ERA for Case 2 are plotted in Figures 6(a) and 6(b), respectively. These figures show all of the modes calculated by each method as the assumed number of modes (an analysis option in both techniques) was incremented from 1 to 64. The identified frequencies are indicated by short, vertical line segments. The height of each line segment is proportional to the corresponding MCF (for Polyreference) or to the corresponding Input Modal Amplitude Coherence (for ERA) calculated for the mode. Both MCF and IMAC are "accuracy indicators" used to help differentiate between extraneous eigenvalues due to noise and data distortions and the actual modes of the system. If the value of the indicator is 100 percent, the corresponding line segment is drawn as long as the distance between tic marks on the vertical axis. All identified eigenvalues are included in these plots; if the indicator had a value of zero, the corresponding mode appears as just a dot in the figure. Numbered arrows at the top of the plots indicate the frequencies selected for the two artificially added modes.

With simple, linear data these plots would also consist of straight, vertical lines located at the natural frequencies of the structure. Any data point falling off the lines would have a small accuracy-indicator value. However, as seen in Figure 6, things are not that straightforward with complex experimental data.

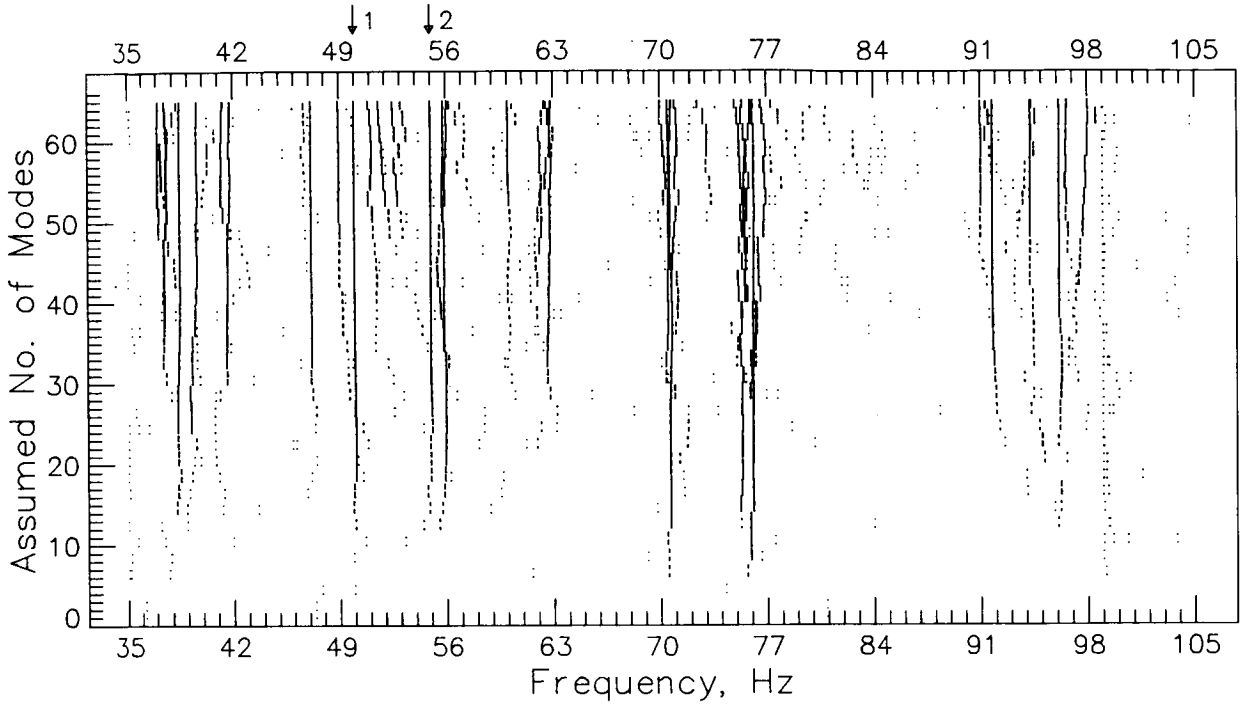

(a) Polyreference Results

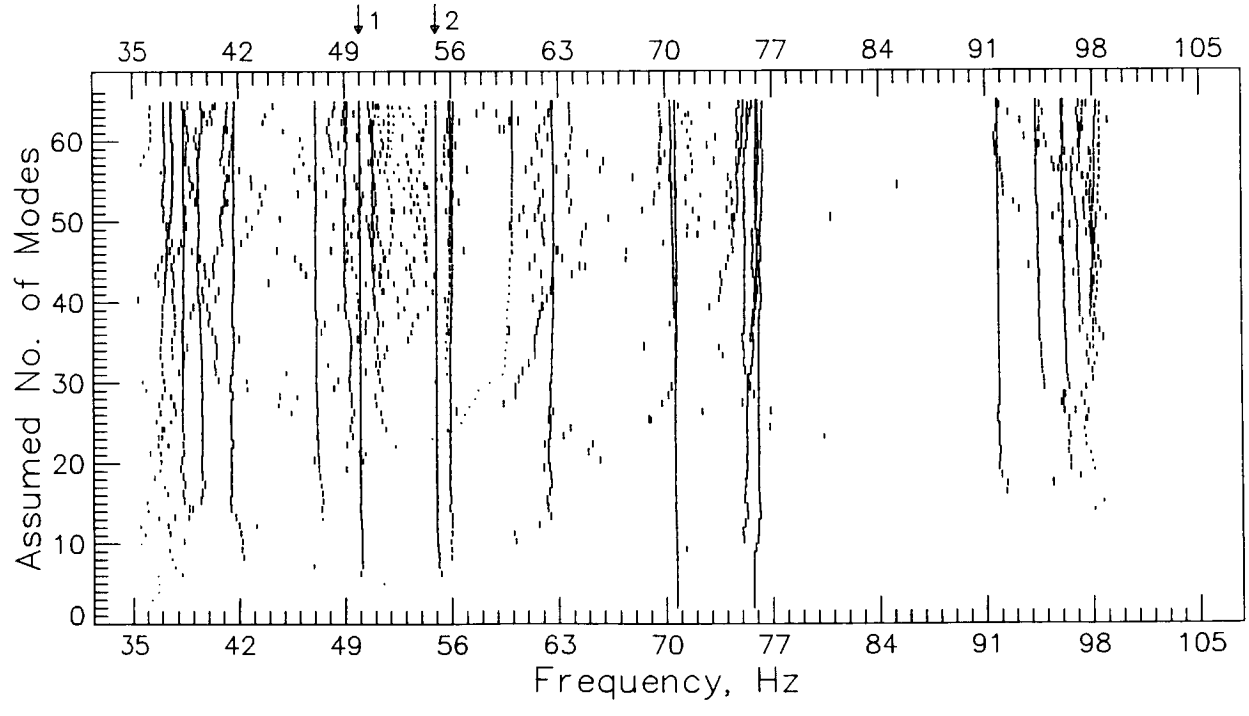

(b) ERA Results

Figure 6. Identified Frequencies for Case 2. Height of Dashed Lines Proportional to MCF (Polyreference) or Input Modal Amplitude Coherence (ERA)

Figures 7 and 8 provide a closer look at the results for Case 2 near the frequency of the second added mode (55 Hz). Figure 7 shows the Polyreference results and Figure 8 the corresponding ERA results. The identified frequencies are shown in the upper-left plots using the same format as in Figure 6. In this case, however, only the results for modes from 53 to 58 Hz are displayed to improve clarity. The five other plots in the figures provide additional, corresponding results for these modes. The true values of each parameter used for the artificial modes are again indicated by numbered arrows above the top axes. The two correlation plots at the bottom of the figures show the square of the correlation coefficient (Ref. 21) between each of the two chosen mode shapes (Figure 5(b)) and each identified shape.

A comparison of Figures 7 and 8 shows that both techniques identified the frequency, damping, residue amplitude, and mode shape information accurately for Case 2 as the assumed number of modes was increased sufficiently, although the rate of convergence is different. However, the identified residue phase angle shows a bias of approximately +15 degrees in both results. The cause of the bias is unknown at this time.

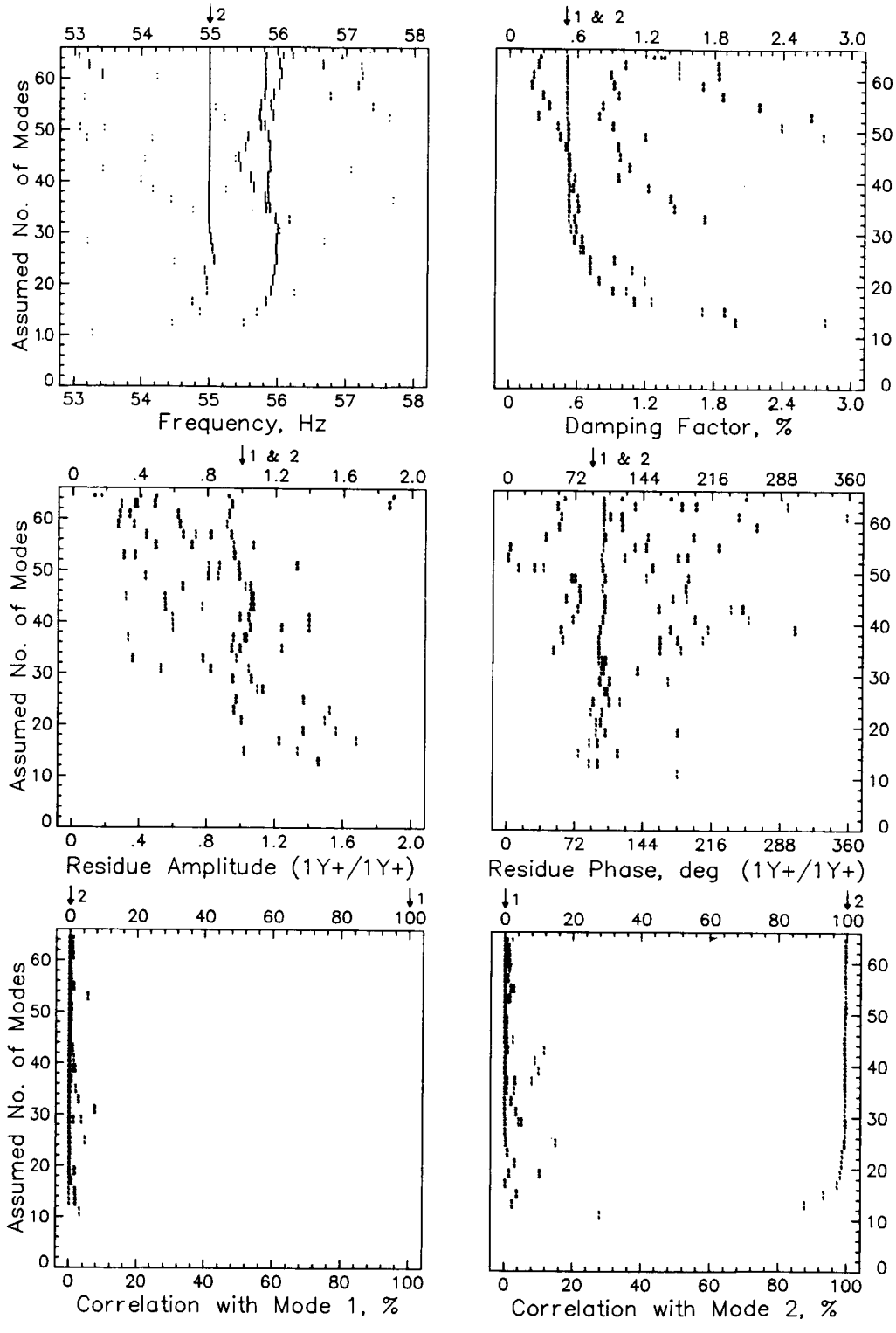

Figure 7. Complete Polyreference Results for Case 2 (Near Frequency of Second Added Mode)

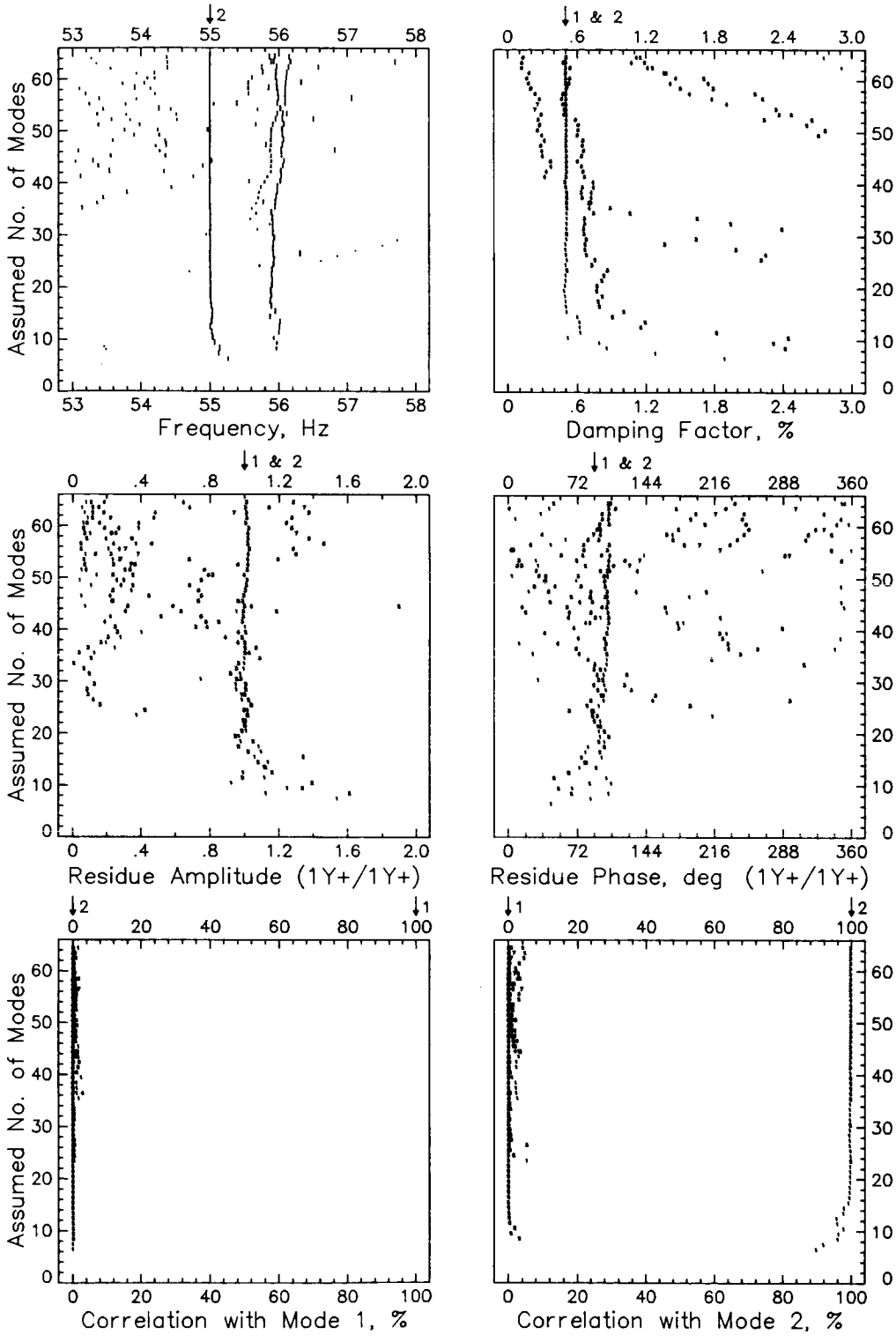

Figure 8. Complete ERA Results for Case 2 (Near Frequency of Second Added Mode)

Additional identification results are provided in Figures 9 and 10 for Cases 3 and 5, respectively. Case 3 used the same parameters as Case 2 except that the residue amplitudes were reduced by a factor of ten. At this low amplitude, the total energy in each of the two added modes is only slightly above the background noise floor. The amplitude reduction has caused the results to be uniformly less accurate than for Case 2. The residue and mode shape results, in particular, show significant deviations from their true values. Also note that the scatter in the frequency and damping results for the weak structural mode at slightly less than 56 Hz is similar in character to that for the 55-Hz artificial mode. This suggests a similar degree of inaccuracy in the identified mode shapes as well.

Figure 10 shows corresponding results for Case 5, in which the frequency of the second added mode was lowered to 50 Hz to generate a repeated eigenvalue. Both techniques successfully identified both modes. Again, however, the convergence rates are different. Note that the residue results are not determined uniquely in this case. The sum of the two identified residues, however, should equal the sum of the two true residues. Note also that the two correlation plots have been replaced by a single plot showing the total correlation between each identified mode shape and the shapes of the two added modes. The total correlation would be 100 percent for each mode for perfect identification.

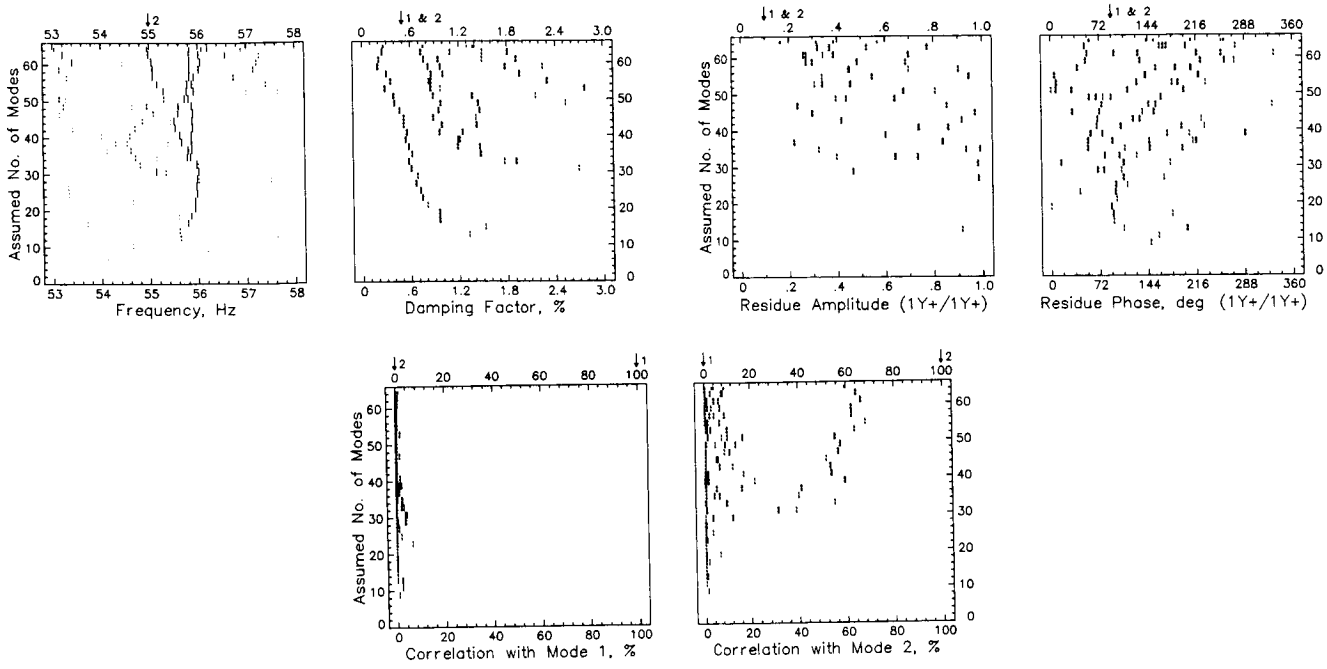

(a) Polyreference

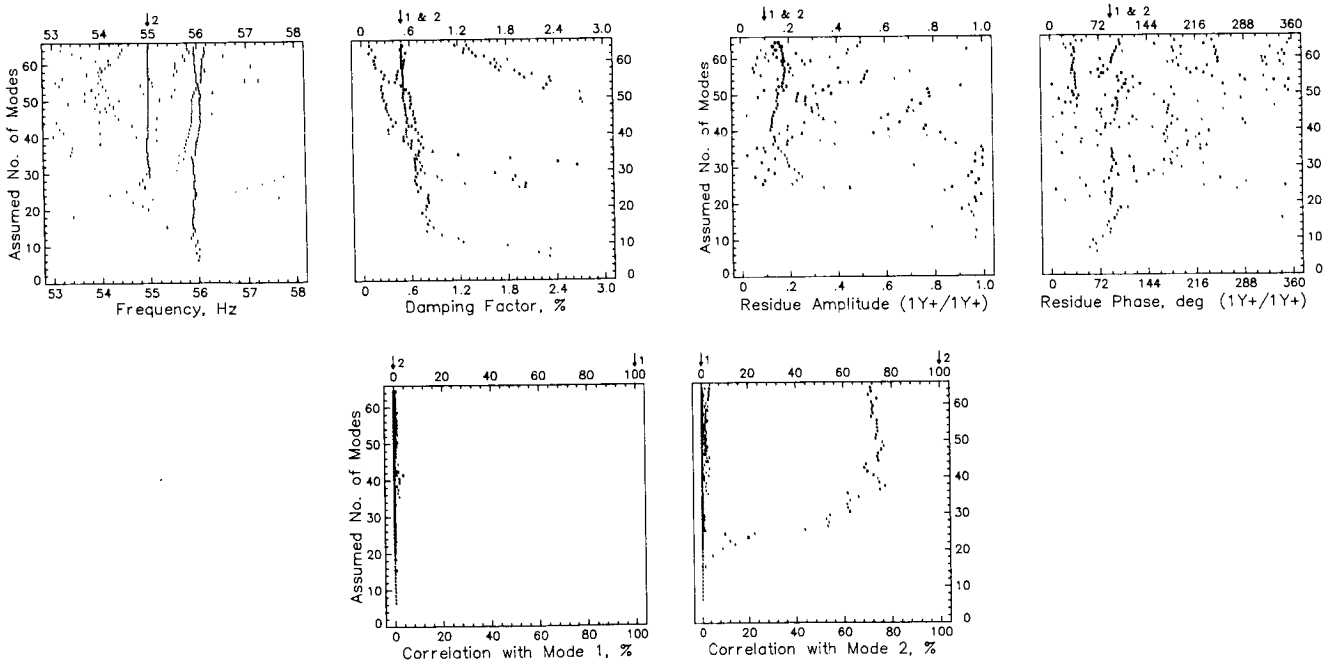

(b) ERA

Figure 9. Results for Case 3

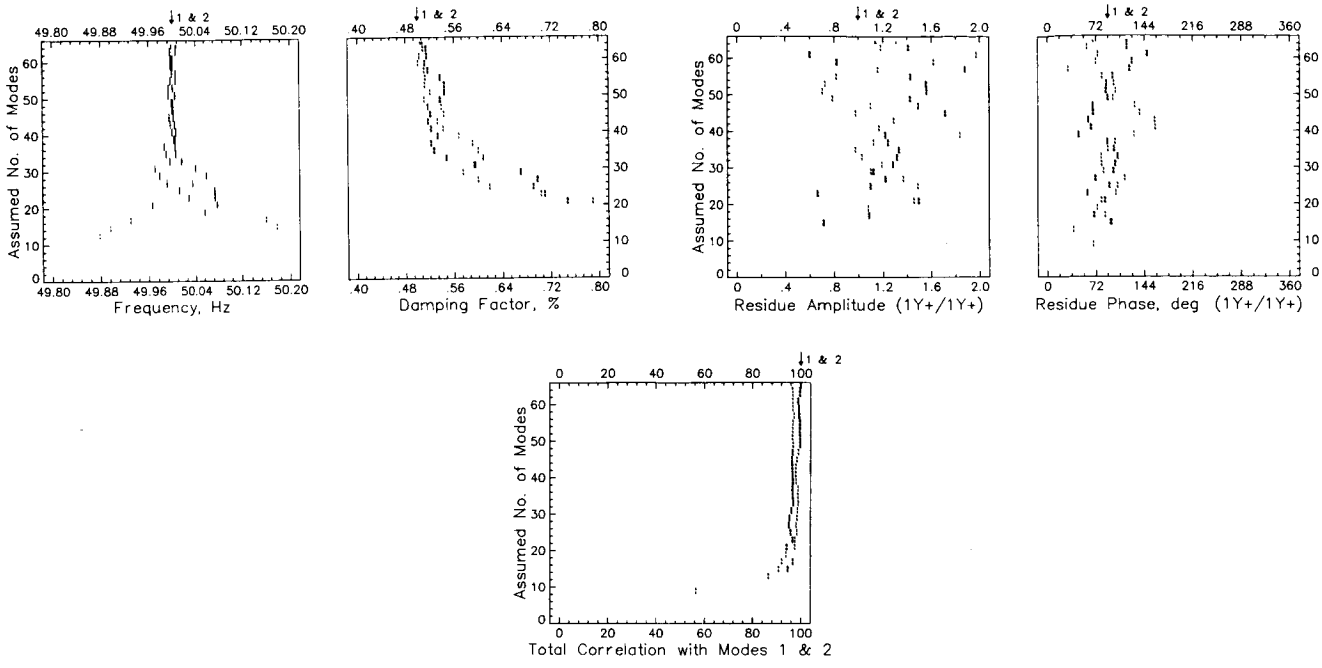

(a) Polyreference

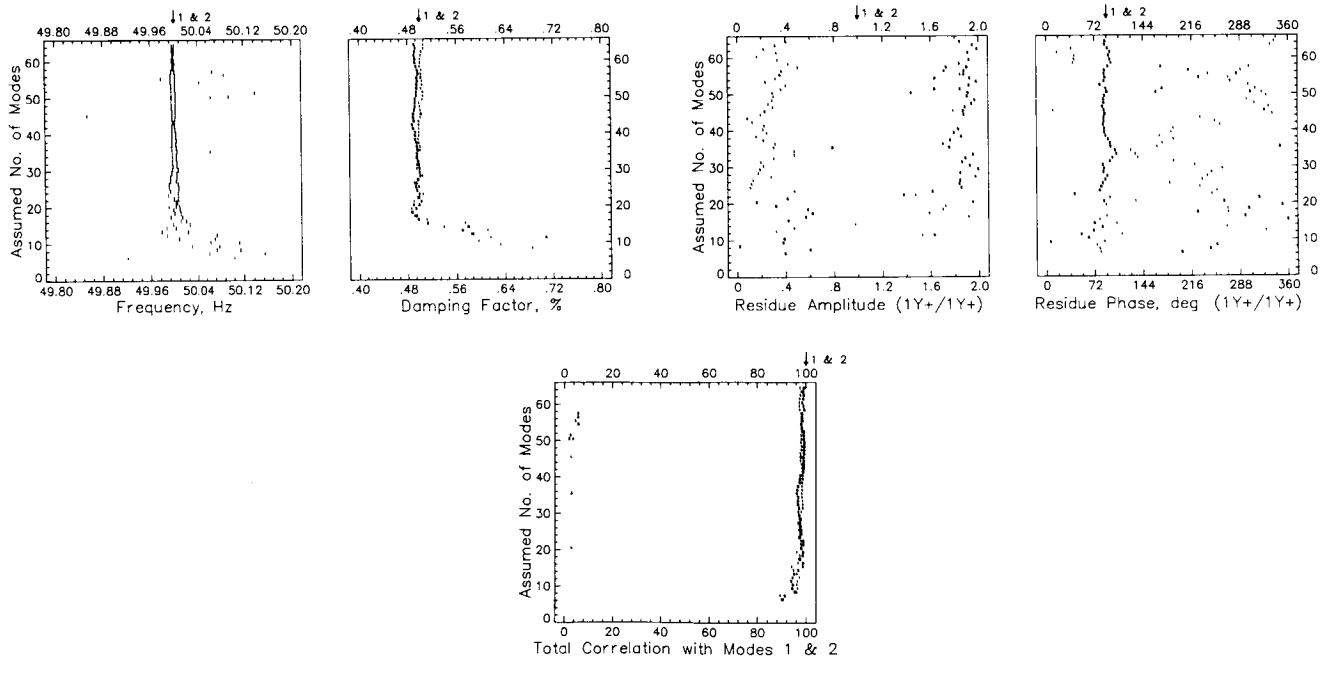

(b) ERA

Figure 10. Results for Case 5

CONCLUDING REMARKS

Modal identification of seemingly simple structures, such as the generic truss discussed in the paper, is often surprisingly difficult in practice due to high modal density, nonlinearities, and other nonideal factors. Under these circumstances, different data analysis techniques can generate substantially different results. This paper summarizes the initial application of a new "hybrid-data" method for studying the performance characteristics of various identification techniques with such data.

This approach offers new pieces of information for the system identification researcher. First, it allows actual experimental data to be used in the studies, while maintaining the traditional advantage of using simulated data. That is, the identification technique under study is forced to cope with the complexities of real data, yet the performance can be measured unquestionably for the artificial modes because their true parameters are known. Secondly, the accuracy achieved for the true structural modes in the data can be estimated from the accuracy achieved for the artificial modes if the results show similar characteristics. This similarity occurred in the study, for example, for a weak structural mode near 56 Hz (ref. Figure 9). It may even be possible--eventually--to use the error information from the artificial modes to improve the identification accuracy for the structural modes.

It must be emphasized, in closing, that it would be premature to generalize the identification results shown in this paper. More work, both numerical and mathematical, is needed to fully characterize the performance of either the Polyreference or the ERA technique with complex experimental data.

REFERENCES

1. Taylor, L. W. and Pinson, L. D., "On-Orbit Identification of Flexible Spacecraft," NASA CP-2368, December 1984, pp. 465-481.

2. Sundararajan, N., Montgomery, R. C., and Williams, J. P., "Adaptive Identification and Control of Structural Dynamics Systems Using Recursive Lattice Filters," NASA TP-2371, January 1985.

3. Mettler, E., Milman, M. H., Rodriguez, G., and Tolivar, A. F., "Space Station On-Orbit Identification and Performance Monitor," AIAA Paper 85-0357, January 1985.

4. Ewins, D. J., Modal Testing: Theory and Practice, John Wiley and Sons, Inc., New York, 1984.

5. Kurdila, A. J. and Craig, R. R., "A Modal Parameter Extraction Procedure Applicable to Linear Time-Invariant Dynamic Systems," Report No. CAR 85-2, Center for Aeronautical Research, The University of Texas at Austin, May 1985.

6. Stroud, R. C., "Excitation, Measurement, and Analysis Methods for Modal Testing," ASCE/ASME Mechanics Conference, Albuquerque, NM, June 1985.

7. Richardson, M. H., "Global Frequency and Damping Estimates from Frequency Response Functions," Fourth International Modal Analysis Conference, February 1986, pp. 465-470.

8. Leuridan, J. M., Brown, D. L. and Allemang, R. J., "Time Domain Parameter Identification Methods for Linear Modal Analysis: A Unifying Approach," AIAA Paper 84-0925, May 1984.

9. Juang, J. N., "Mathematical Correlation of Modal Parameter Identification Methods Via System Realization Theory," NASA TM-87720, April 1986.

10. Vold, H., Kundrat, J., Rocklin, G. T., and Russell, R., "A Multi-Input Modal Estimation Algorithm for Mini-Computers," SAE Paper 820194, February 1982.

11. Vold, H. and Russell, R., "Advanced Analysis Methods Improve Modal Test Results," Sound and Vibration, March 1983, pp. 36-40.

12. Crowley, J. R., Hunt, D. L., Rocklin, G. T., and Vold, H, "The Practical Use of the Polyreference Modal Parameter Estimation Method," Second International Modal Analysis Conference, February 1984, pp. 126-133.

13. Vold, H. and Crowley, J. R., "A Modal Confidence Factor for the Polyreference Method," Third International Modal Analysis Conference, January 1985, pp. 305-310.

14. Juang, J. N. and Pappa, R. S., "An Eigensystem Realization Algorithm for Modal Parameter Identification and Model Reduction," J. Guidance, Control and Dynamics, Vol. 8, Sept.-Oct. 1985, pp. 620-627.

15. Pappa, R. S. and Juang, J. N., "Galileo Spacecraft Modal Identification Using an Eigensystem Realization Algorithm," J. of the Astronautical Sciences, Vol. 33, Jan.-March 1985, pp. 15-33.

16. Brumfield, M. L., Pappa, R. S., Miller, J. B., and Adams, R. R., "Orbital Dynamics of the OAST-1 Solar Array Using Video Measurements," AIAA Paper 85-0758, April 1985.

17. Juang, J. N. and Pappa, R. S., "Effects of Noise on Modal Parameters Identified by the Eigensystem Realization Algorithm," J. Guidance, Control and Dynamics, Vol. 9, May-June 1986, pp. 294-303.

18. Zimmerman, R. and Hunt, D. L., "Multiple-Input Excitation Using Burst Random for Modal Testing," Sound and Vibration, October 1985, pp. 12-21.

19. Vold, H., Crowley, J. R., and Rocklin, G. T., "New Ways of Estimating Frequency Response Functions," Sound and Vibration, November 1984, pp. 34-38.

20. Structural Dynamics Research Corporation and CAE International, Modal-Plus Reference Manual, Version 9.0, 1985.

21. Allemang, R. J. and Brown, D. L., "A Correlation Coefficient for Modal Vector Analysis," First International Modal Analysis Conference, November 1982, pp. 110-116.